

## 3-D Numerical and Experimental Study of the Turbulent Mixing Layer between Two Non-Parallel Streams\*

Asst. Prof. Dr. Jalal M. Jalil  
Educational Technology Department  
University of Technology, Baghdad, Iraq

Asst. Prof. Dr. Talib K. Murtagha  
Mechanical Engineering Department  
University of Technology, Baghdad, Iraq

Dr. Khudheyer S. Mushatet  
Mechanical Engineering Department  
University of Technology, Baghdad, Iraq

### Abstract

Results of numerical and experimental study on the turbulent mixing layer of three-dimensional non-parallel streams are reported. The numerical prediction was based on  $k-\epsilon$  model. Fully elliptic Navier Stokes and energy equations are solved using finite difference primitive variables method. The study has been carried out at Reynolds numbers,  $Re = 19200, 28000, 48000$ , and three velocity ratios  $U_1/U_2$  of 0.3, 0.5, and 1.0. The flow studied. The mean velocity and temperature profiles are studied up to 42 orifice width down stream from the of the high speed side is heated and the flow of the low speed side is kept at room temperature.

Two interception angles of  $(12.5^\circ, 25^\circ)$  were orifice. The results show that there was significant effect of the angle and the mixing ratio on the characteristics of the flow field. The two jets are merged upstream of their geometric interception. The centerline of the combined jet is tilted from the midline between the two orifices when the two jets have different velocities at the large interception angle. Also the results indicated that the mixing layer penetrated deeper into the low speed side than into the high speed of the flow. The numerical results are compared with the experimental results and found to be in moderate agreement.

### الخلاصة

درست طبقة الخلط الاضطرابية الناتجة من تداخل نفائين غير متوازيين بثلاثة أبعاد. استخدام نموذج الاضطراب ( $k-\epsilon$ ) لدراسة تأثير الاضطراب على الجريان وأستخدمت طريقة (Patankar) لحل معادلات (Navier-Stokes) ومعادلة الطاقة. أرقام رينولد المدموسة تراوحت بين (1-0.3). تم تسخين المائع ذو السرعة العالية وثبتت درجة حرارة المائع ذو السرعة الواطئة بدرجة حرارة الغرفة. زاويتي التقاطع المدموسة بين النفائين كانتا  $(12.5^\circ-25^\circ)$ . منحنيات السرعة ودرجات الحرارة درست الى مديات وصلت 42 مرة بقدر عرض فتحة النفث. أستنتج من تحليل النتائج أن محور النفث المتحد يكون مائلا عن الخط الوسطي بين مركزي الفتحتين عندما يختلف النفائين بنسب السرعة وعند زاوية التقاطع الكبيرة، كما بينت النتائج أن طبقة الخلط إنتشرت بصورة أكبر عند جانب الجريان ذو السرعة الواطئة أكثر من جانب الجريان ذو السرعة العالية. قورنت النتائج العددية مع النتائج العملية وكان التوافق متوسطا.

### 1. Introduction

The mixing of jets is of practical importance in a wide variety of applications. It is used, for example, in powered high-lift systems of aircraft, burners, and fluidic devices. The mixing of jets has been examined experimentally and theoretically [1-5]. In these studies the spacing  $S$  and the angle of interception of the two jets affected the characteristics of the flow field. The present work is directed toward examining the flow field generated by the interaction of two non-parallel streams for an interception angles of (12.5, 25) and velocity ratios of (0.3,0.5,1).

Experiments were conducted with one of the jets having a specified velocity and temperature while the velocity of the heated jet was adjusted such that  $U_1/U_2$  had different values between 0, 1.

The algorithm SIMPLE [6] was used in this paper to study the problem with the Navier-Stokes equations written in terms of primitive variable method (U, V, P).

## 2. Apparatus and Procedure

A schematic representation of the problem is shown in **Fig.(1)**. The variable speed blower was used to provide the airflow to the two identical separate rectangular orifice jets. The orifice has a width ( $h$ ) of 4cm and a depth ( $b$ ) of 12cm, (i.e. the aspect ratio,  $b/h$  is 3). The distance  $S$ , between centers of the two orifices is  $S/h=1.4$  for  $\psi=12.5\text{deg}$ . and  $S/h=1.6$  for  $\psi=25\text{deg}$ . The facility is designed such that the two jets can be interacting at various interception angles. The measurements were made with a pitote static tube connected to digital micromanometer for measuring the velocity and thermocouple connected to digital thermometer for measuring the temperature.

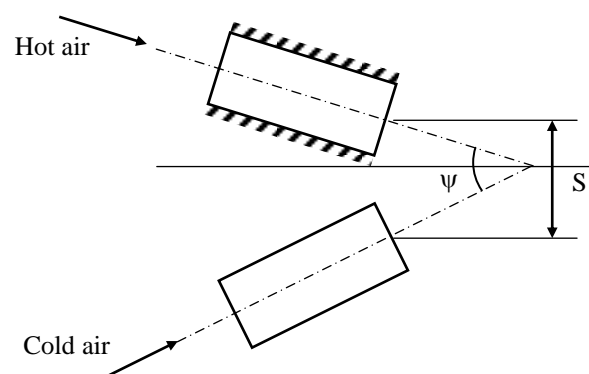


**Figure (1) Configuration of the problem**

### 3. Theory

#### 3-1 Mean Flow Equations

The flow is assumed to be three-dimensions with constant properties, and the buoyancy effect is neglected. The mean flow equations for continuity, momentum and energy may be expressed for steady state conditions in the following conservative form <sup>[6,7]</sup> as:

$$\frac{\partial U}{\partial x} + \frac{\partial V}{\partial y} + \frac{\partial W}{\partial z} = 0 \dots\dots\dots (1)$$

$$U \frac{\partial U}{\partial x} + V \frac{\partial U}{\partial y} + W \frac{\partial U}{\partial z} = -\frac{\partial P}{\partial x} + \nu_{eff} \nabla^2 U + \nu_{eff} \left( \frac{\partial^2 U}{\partial x^2} + \frac{\partial^2 V}{\partial x \partial y} + \frac{\partial^2 W}{\partial x \partial z} \right) \dots\dots\dots (2)$$

$$U \frac{\partial V}{\partial x} + V \frac{\partial V}{\partial y} + W \frac{\partial V}{\partial z} = -\frac{\partial P}{\partial y} + \nu_{eff} \nabla^2 V + \nu_{eff} \left( \frac{\partial^2 U}{\partial x \partial y} + \frac{\partial^2 V}{\partial y^2} + \frac{\partial^2 W}{\partial y \partial z} \right) \dots\dots\dots (3)$$

$$U \frac{\partial W}{\partial x} + V \frac{\partial W}{\partial y} + W \frac{\partial W}{\partial z} = -\frac{\partial P}{\partial z} + \nu_{eff} \nabla^2 W + \nu_{eff} \left( \frac{\partial^2 U}{\partial x \partial z} + \frac{\partial^2 V}{\partial y \partial z} + \frac{\partial^2 W}{\partial z^2} \right) \dots\dots\dots (4)$$

$$U \frac{\partial T}{\partial x} + V \frac{\partial T}{\partial y} + W \frac{\partial T}{\partial z} = \Gamma_e \nabla^2 T \dots\dots\dots (5)$$

where:

$$\frac{\partial^2}{\partial x^2} + \frac{\partial^2}{\partial y^2} + \frac{\partial^2}{\partial z^2} = \nabla^2 \dots\dots\dots (6)$$

#### 3-2 Turbulence Model

##### 3-2-1 The Standard k-ε Model

The k-ε model characterizes the local state of turbulence by two parameters: the turbulent kinetic energy, k, and the rate of its dissipation, ε.

The turbulent viscosity is related to these parameters by the Kolmogorov-Prandtl expression:

$$\nu_t = C_\mu \frac{k^2}{\epsilon} \dots\dots\dots (7)$$

where:  $c_\mu$ : is an empirical constant.

The distribution of  $k$  and  $\varepsilon$  over the flow field is calculated from the following semi-empirical transport equations for  $k$  and  $\varepsilon$ :

$$\frac{\partial U k}{\partial x} + \frac{\partial V k}{\partial y} + \frac{\partial W k}{\partial z} = \frac{v_t}{\sigma k} \nabla^2 k + v_t \left[ 2 \left( \frac{\partial U}{\partial x} \right)^2 + 2 \left( \frac{\partial V}{\partial y} \right)^2 + 2 \left( \frac{\partial W}{\partial z} \right)^2 + \left( \frac{\partial U}{\partial y} + \frac{\partial V}{\partial x} \right)^2 + \left( \frac{\partial U}{\partial z} + \frac{\partial W}{\partial x} \right)^2 + \left( \frac{\partial V}{\partial z} + \frac{\partial W}{\partial y} \right)^2 \right] - \varepsilon \quad \dots (8)$$

$$\frac{\partial U \varepsilon}{\partial x} + \frac{\partial V \varepsilon}{\partial y} + \frac{\partial W \varepsilon}{\partial z} = \frac{v_t}{\sigma \varepsilon} \nabla^2 \varepsilon + v_t C_{1\varepsilon} \frac{\varepsilon}{k} \left[ 2 \left( \frac{\partial U}{\partial x} \right)^2 + 2 \left( \frac{\partial V}{\partial y} \right)^2 + 2 \left( \frac{\partial W}{\partial z} \right)^2 + \left( \frac{\partial U}{\partial y} + \frac{\partial V}{\partial x} \right)^2 + \left( \frac{\partial U}{\partial z} + \frac{\partial W}{\partial x} \right)^2 + \left( \frac{\partial V}{\partial z} + \frac{\partial W}{\partial y} \right)^2 \right] - C_{2\varepsilon} \frac{\varepsilon^2}{k} \quad \dots (9)$$

where: empirical constants in the above model are:  $c_{\mu}=0.09$ ,  $\sigma_k=1$ ,  $\sigma_{\varepsilon}=1.3$ ,  $c_{1\varepsilon}=1.44$ ,  $c_{2\varepsilon}=1.92$ .

### 3-2-2 Boundary Conditions

#### *At the Free Edges:*

$\partial U/\partial y = 0$ ;  $\partial V/\partial y = 0$  ;  $\partial W/\partial y = 0$  ;  $\partial T/\partial y = 0$  ;  $k = \varepsilon = 0$ . The stream wise pressure gradient ( $\partial p/\partial x$ ) originally appearing in eq.(2) is negligible (The surrounding are at rest).

#### *Numerical Solution:*

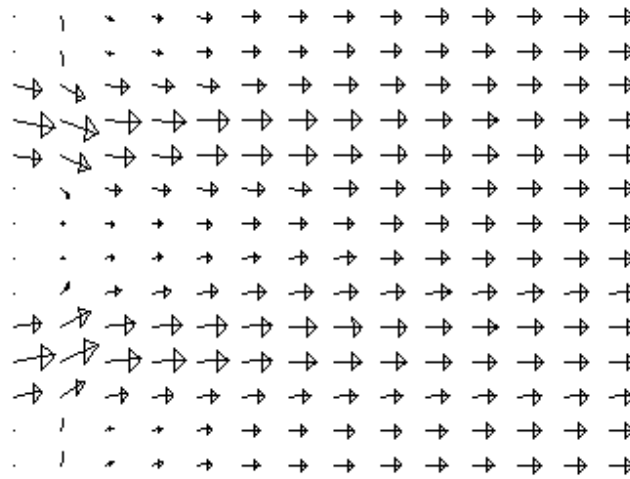
Numerical procedure called SIMPLE (semi-implicit method for pressure-linked equations) is used to solve the basic conservative equations. Full detailed is found in ref.[6].

## 4. Results and Discussion

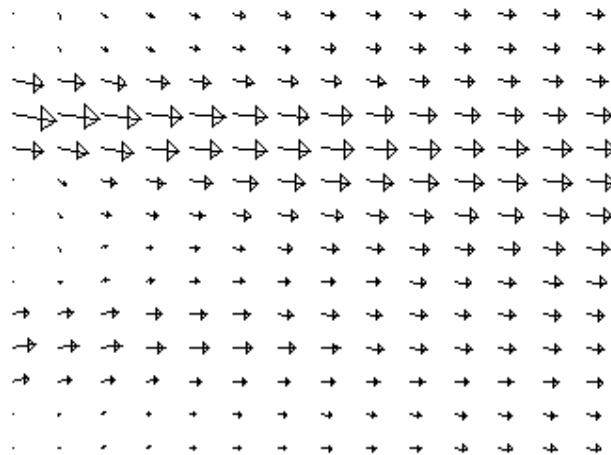
Results are obtained numerically and experimentally for incompressible flow under the conditions illustrated in the forgoing sections. The flow field and thermal characteristics for different Reynolds numbers, different velocity ratios, and different interception angles are discussed separately.

Effects of velocity ratio and the angles of interception on the flow field characteristics are clearly seen in **Figs.(2-3)**.

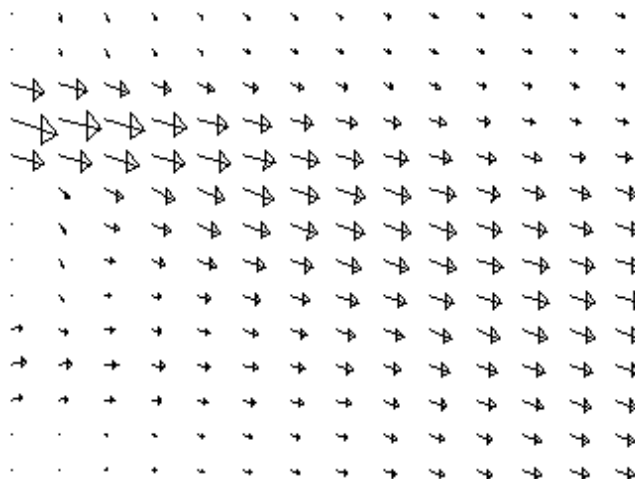
The combined jet centerline is tilted from the midline between the two orifices when the two jets have different velocity and this effect is increased at the large interception angle especially at ( $V_R=0.3$  and  $\psi=25^\circ$ ) because of the increase of the component of velocity towards the y-axis. The decay of axial velocity at the interception angle of 25 is higher than that of the angle of 12.5. As the **Figs.(2-3)** show, the two jet merge upstream of their geometric interception at both the angle of interceptions because the mutual entrainment of the surrounding air creates a sub atmospheric region between the two jet and that cause them to merge upstream of their geometric interception. The growth of the mixing layer is found to be linear at both cases.



(a)

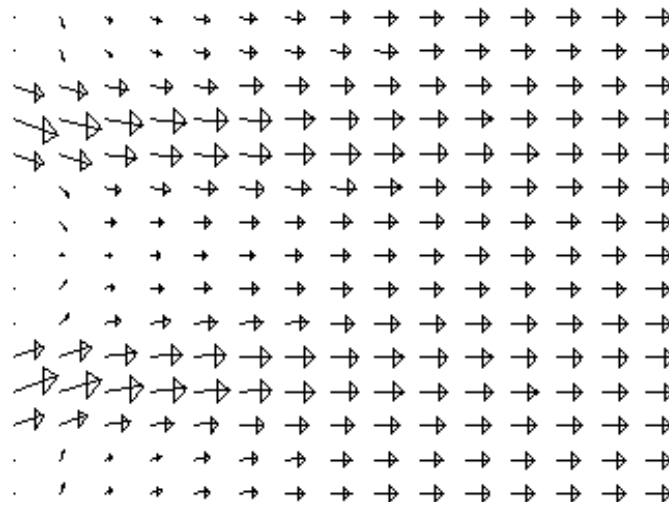


(b)

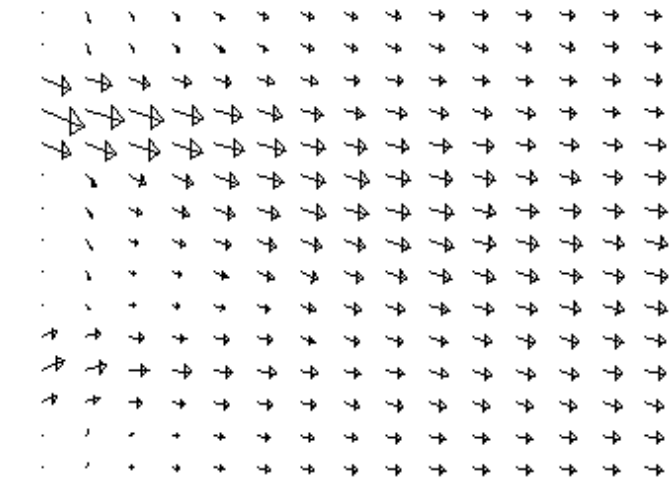


(c)

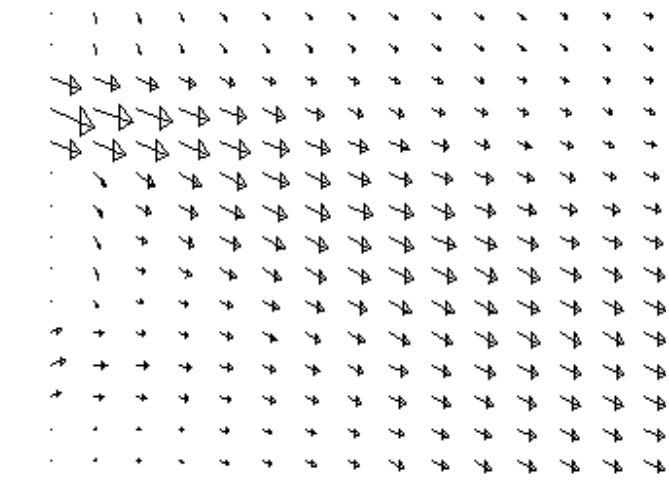
Figure (2) Turbulent flow field (U&V velocity vectors) for different velocity ratios (a.  $V_R=1.$ , b.  $V_R=0.5$ , c.  $V_R=0.3$ ) and  $\psi=12.5$



(a)



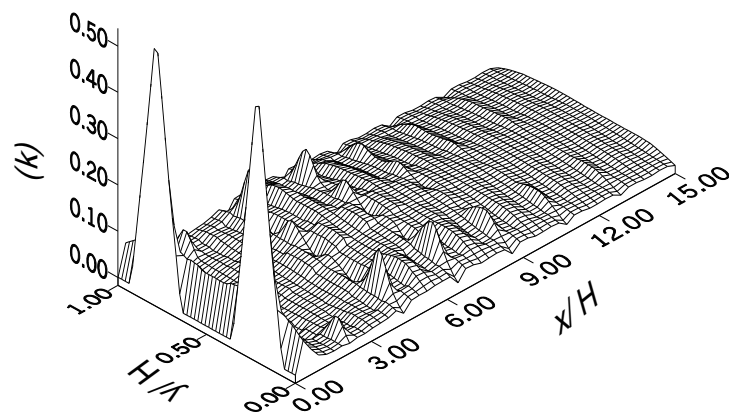
(b)



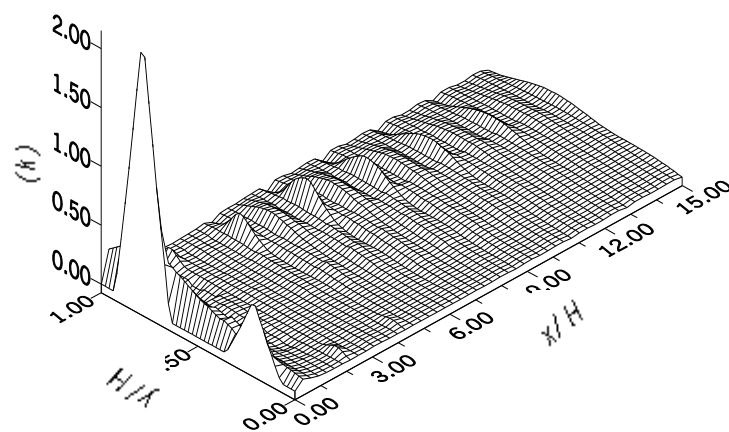
(c)

Figure (3) Turbulent flow field (U&V velocity vectors) for different velocity ratios (a.  $V_r=1.$ , b.  $V_r=0.5$ , c.  $V_r=0.3$ ) and  $\psi = 25$

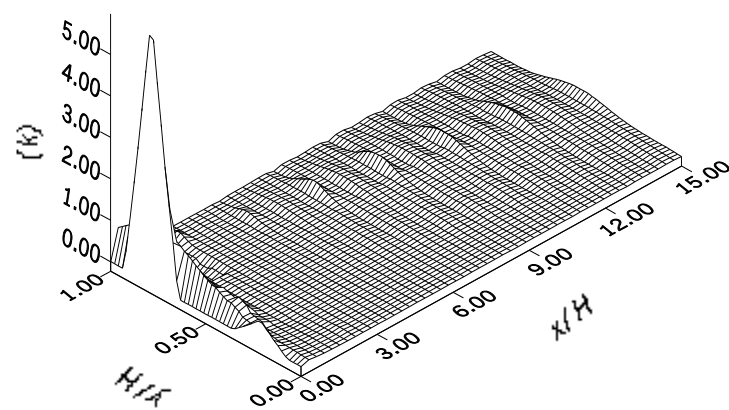
**Figure (4)** exhibited the turbulent kinetic energy distribution at different velocity ratios. The two peaks of the two jets decay rapidly and spread with down stream distance in the region when the two jets combined. It is noted that there are significant differences in the distribution for different velocity ratios. These may be attributed to differences in production, transport and dissipation of turbulent kinetic energy between the two peaks of the two jets associated with different velocity ratios and different angles of interception.



(a)



(b)



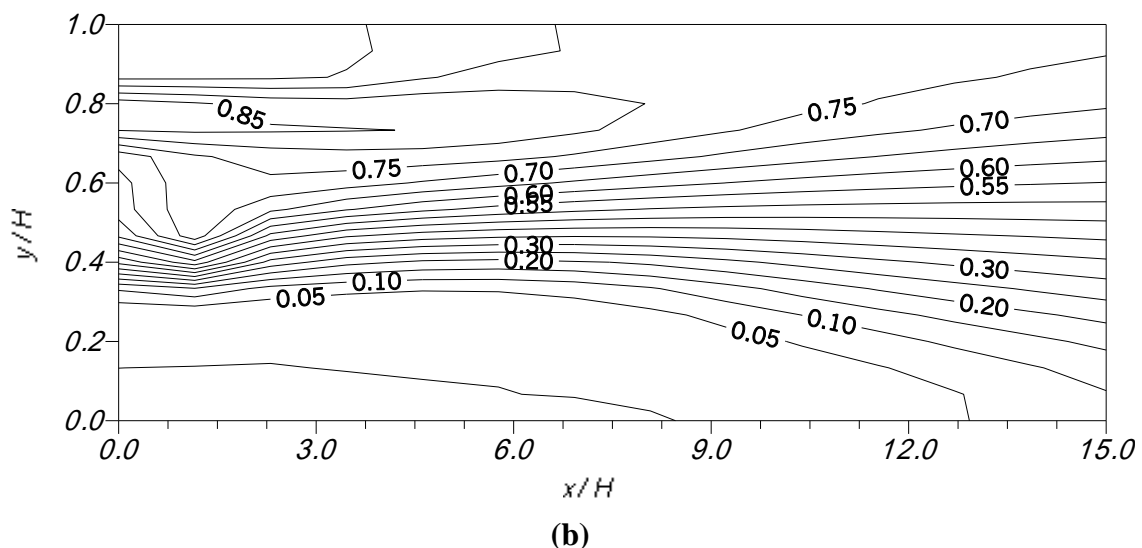
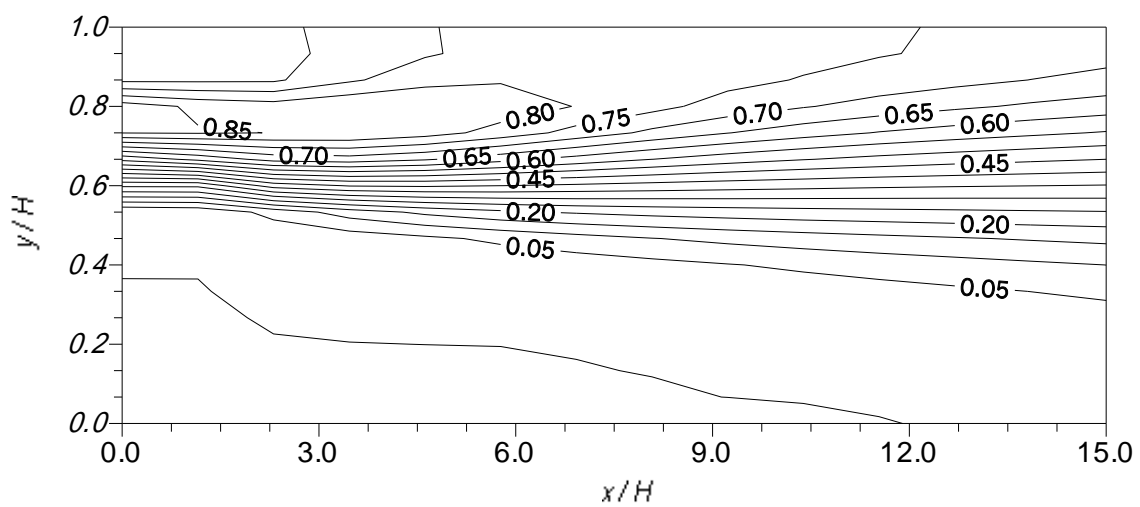
(c)

**Figure (4)** distribution of turbulent kinetic energy for different velocity ratios  
a.  $V_R=1$  , b.  $V_R=0.5$  , c.  $V_R=0.3$

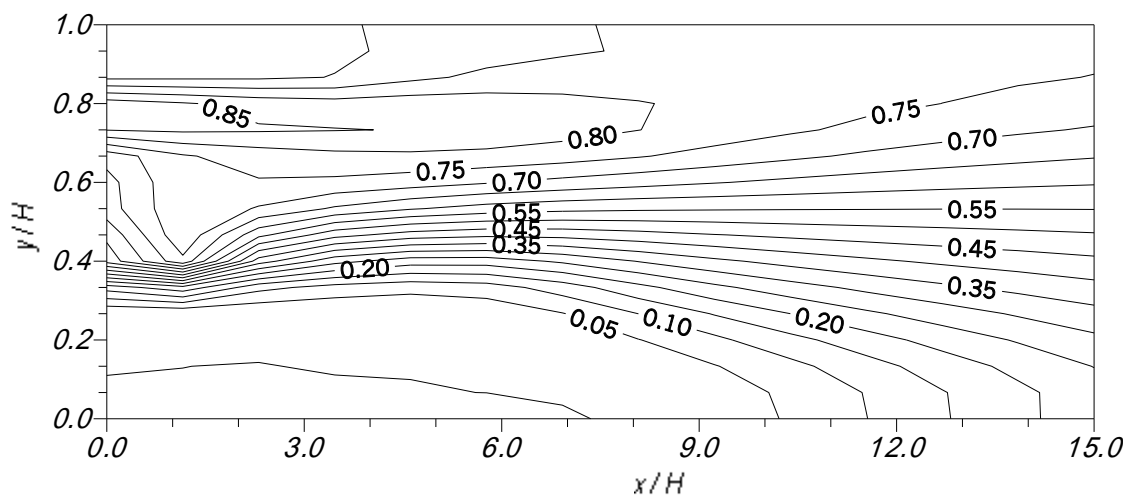
## 5. Thermal Characteristics

The predicted isotherm contours are illustrated in **Figs.(5-6)** for different velocity ratios and different interception angles. The results show the decay of axial temperature for the above cases due to interchange of energy between the two streams and the surrounding. The turbulent transport of thermal energy is slower than that of momentum. The secondary flow temperatures between the two streams create a distortion in thermal layers of the two jets and that differs from the angle to other due to the difference in the geometric interception.

The computed mean velocity and temperature profiles at different axial locations away from the orifice exit plane are compared with the experimental data and are shown in **Fig.(7)**. The agreement is found to be moderate.

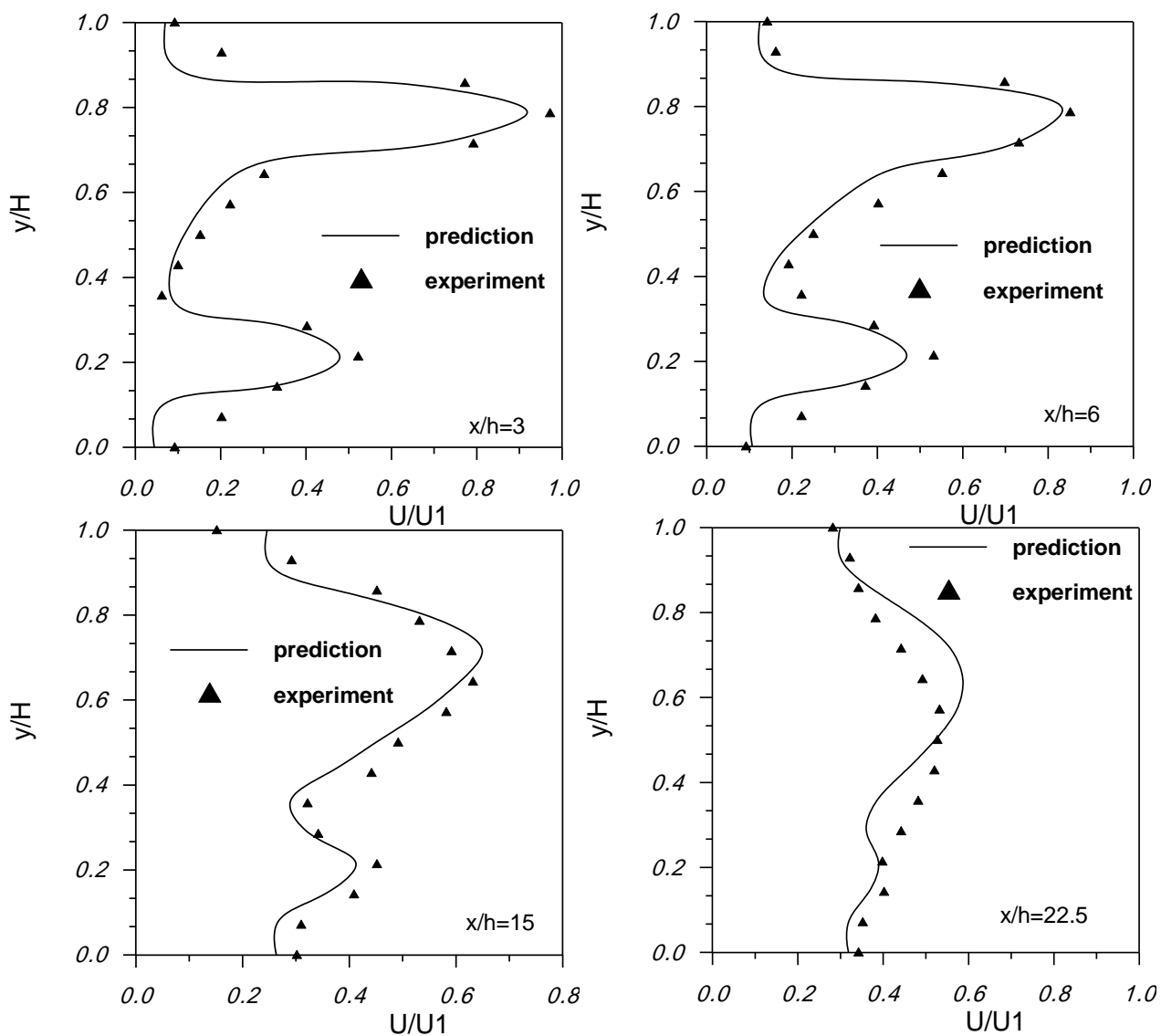






(c)

Figure (5) Isotherm temperature contours for  $\psi = 12.5$  and for different velocity ratios, a.  $V_R = 1$ , b.  $V_R = 0.5$ , c.  $V_R = 0.3$



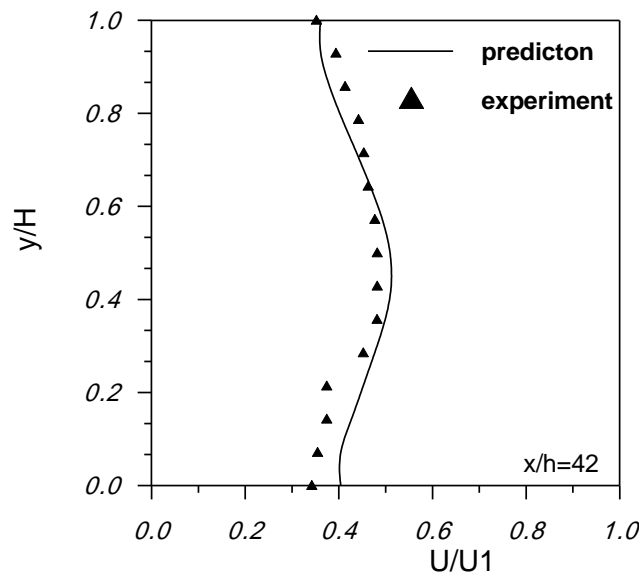


Figure (7) Comparison of predicted and experimental results at different axial locations for  $V_R=0.5$  and  $\psi=25$  deg

## 6. Conclusions

Numerical and experimental investigation of three-dimensional mixing layer between non-parallel streams is obtained. The study is performed for different velocity ratios and different angles of interceptions with Reynolds numbers up to  $4.8 \times 10^4$   $k-\epsilon$  capability for modeling incompressible free shear flows has been validated against experimental measurements. The prediction of mixing layer growth and its turbulent characteristics are in moderated agreement with experimental data.

## 7. References

1. Krothapalli, A., Baganoff, D., and Karmancheti, K., *"The Development and Structure of a Rectangular Jet in a Multiple Jet Configuration"*, AIAA Journal, Vol. 18, Aug. 1980, pp. 645-650.
2. Marstes, G. F., *"Interaction of Two Plane Parallel Jets"*, AIAA Journal, Vol. 15, No. 12, December 1977.
3. Foss, J. F., *"Flow Characteristics of the Defined Region Geometry for High-Gain Proportional Amplifiers"*, Proceeding of 1967 Fluidic Symposium, The American Society of Mechanical Engineering, Chicago, May 1967, pp. 45-61.
4. Elbanna, H., Gahin, S., and Rashid, M. I. I., *"Investigation of Two Plane Parallel Jets"*, AIAA Journal, Vol. 21, July 1983, pp. 985-986.

5. Jones, W. P., and Lunder, B. E., “*The Prediction of Laminarization with a Two Equation Model of Turbulence*”, Journal of Heat and Mass Transfer, Vol. 15, 1972, pp. 301-314.
6. Patankar, S. V., “*Numerical Heat Transfer and Fluid Flow*”, McGraw-Hill, New York, 1980.
7. Versteeg, H. K., and W., Malasekera, “*An Introduction to Computational Fluid Dynamics*”, Longman Group ltd, 1995.

### Notations

B	Orifice breadth, m
$C_{\mu}$ , $C_{1\varepsilon}$ , $C_{2\varepsilon}$	Constants in turbulence model
$D_h$	Hydraulic diameter, m
$A_R$	Aspect ration of jet = b/h
h	Width of orifice, m
k	Turbulent Kinetic energy = $\frac{1}{2} \left( \overline{u'^2} + \overline{v'^2} + \overline{w'^2} \right)$ , $m^2/s^2$
P	Mean static pressure, $N/m^2$
Re	Reynolds number = $\frac{U_{av1} \cdot h}{\nu}$
S	Distance between the centers of the two orifices, m
U	Mean velocity in the x-direction, m/s
$U_1$	Mean velocity of higher velocity jet, m/s
$U_2$	Mean velocity of lower velocity jet, m/s
V	Mean velocity in the y-direction, m/s
$V_R$	Velocity ratio ( $U_{av2}/U_{av1}$ )
W	Mean velocity in the z-direction, m/s
x, y, z	Cartesian Coordinates, m

### Greek

$\theta$	Dimensionless temperature,
$\psi$	Angle of interception of the two jets, deg.
$\nu$	Kinematic viscosity, $m^2/s$
$\nu_e$	Effective Kinematic viscosity, $m^2/s$
$\varepsilon$	Dissipation of turbulent kinetic energy, $m^2/s^3$
$\sigma_k$ , $\sigma_\varepsilon$	Turbulent prandtl numbers for k, $\varepsilon$
$\Gamma$	Diffusion coefficient, $N.s/m^2$
$\Gamma_e$	Effective diffusion coefficient, $N.s/m^2$